Chapter 2

Ising ferromagnet driven by propagating and standing magnetic wave.

2.1 Introduction:

The hysteretic response and the nonequilibrium phase transition [1, 2, 3] of a 2D Ising ferromagnet driven by uniformly oscillating magnetic field has been discussed mainly in the previous chapter. In those discussions, it is seen that the driving magnetic field, which takes the ferromagnet away from equilibrium, varies only in time. There is no spatial variation of magnetic field at a particular time throughout the whole lattice, i.e. the magnetic field remains uniform over the whole lattice at any particular instant. The situation becomes quite interesting when the driving field varies in space as well as in time. In reality, when a magnetic wave passes through a ferromagnet, all the spins in the ferromagnet do not feel the same influence of the magnetic field at a particular instant. Also such a kind of varying (in both space and time) magnetic field, when couples with the spins of the ferromagnet, affects the dynamic response of the system. The dynamic phase transition, observed here, also show some new characteristic behavior in the dynamical patterns of the phase of the system. I have mentioned few studies with spatio-temporal variation [4, 5] of magnetic field in the previous chapter. Here, I am going to address the nonequilibrium behaviors leading to phase transition occurred in a 2D Ising ferromagnet under spatio-temporal variation of magnetic field, mainly in the form of magnetic wave such as propagating magnetic wave and standing magnetic wave. These results for propagating magnetic wave and standing magnetic wave were published in the journals, the full reference of which are respectively:

Muktish Acharyya *Acta.Phys.Polon.B.* **45**(2014)1027

Ajay Halder and **Muktish Acharyya** *J.Magn.Magn.Mater.* **420**(2016)290

2.2 Driven Ising($S = \frac{1}{2}$) ferromagnet:

In an Ising ferromagnet [6] spins orient in two directions either up or down. The magnetic field, of magnetic wave passing through the ferromagnet, tries to orient the ferromagnetic spins of the system towards its direction which reverses at every interval of half time period of the magnetic oscillations. The ferromagnetic interaction between the spins competes with this effort of the magnetic perturbation and tries to resist against the fluctuation of spins. At higher temperatures thermal fluctuations of spins increase and effect of magnetic perturbation is more pronounced within the system. Depending upon

the strength of magnetic field i.e. the field amplitude, frequency of magnetic oscillations of spins and the temperature of the system different dynamical phases are observed to exist.

2.2.1 Response to propagating magnetic wave:

The time dependent Hamiltonian of the two-dimensional Ising ferromagnet (having uniform nearest neighbor interaction) in the presence of an magnetic field wave (having spatio-temporal variation) can be expressed as-

$$H(t) = -J\Sigma\Sigma' s^z(x,y,t)s^z(x',y',t) - \Sigma h^z(x,y,t)s^z(x,y,t). \tag{2.1}$$

The first term represents the spin-spin interaction energy whereas the other term is the spin-magnetic field interaction energy. $s^z(x,y,t)$ is the Ising *spin variable* (± 1) at lattice site (x,y) at time t. $+1$ refers to the up spin state whereas -1 refers to the down spin state. The summation Σ' extends over the nearest neighbor sites (x',y') of given site (x,y) and the summation Σ extends over all the lattice sites (x,y). $J(>0)$, represents the *ferromagnetic spin-spin interaction strength* between the nearest neighbors. For simplicity, the value of J is considered to be uniform over the whole lattice. $h^z(x,y,t)$ is the *magnetic field* at site (x,y) at time t, which has the following form of Propagating wave,

$$h^z(x,y,t) = h_0 cos(2\pi ft - 2\pi\frac{y}{\lambda}) \tag{2.2}$$

h_0, f and λ represent respectively *the field amplitude, the frequency of magnetic field oscillation and the wavelength* of the propagating magnetic wave. Here, the magnetic wave is assumed as *linearly polarized* along the direction parallel to the spins (s^z). Above form of wave indicates that the wave is propagating towards positive y- direction.

Monte-Carlo Simulation:

The dynamics of spin patterns and their evolution may be achieved through Monte-Carlo simulation [7]. The well known technique of *Monte-Carlo* (MC) method is most useful in studying such dynamics. In this present study, an $L \times L$ square lattice is considered over which an L^2 number of spins are arranged. L represents the linear dimension of the square lattice. The boundary condition is kept periodic in both directions. Such a boundary condition preserves the translational invariance throughout the lattice.

Now, to start with MC technique it is necessary to define the initial spin configuration. Here the initial ($t = 0$) configuration is chosen as the half of the total number of spins (selected at random) are up ($s^z(x, y, t) = +1$) and the others are down ($s^z(x, y, t) = -1$). This represents high temperature paramagnetic phase. The system is now cooled down from such high temperature random configuration. The spins are updated randomly according to the *Metropolis rate (W)* [7] given by,

$$W(s^z \rightarrow -s^z) = Min[exp(-\Delta E/kT), 1] \tag{2.3}$$

where ΔE is the change in energy due to spin flip and k is the Boltzmann constant. The nonequilibrium steady state is the state where the value of each dynamical variable, describing the spin state, is almost independent of time. For this the system is kept in a heat bath at a constant temperature for a long time. The time, measured here, is in the standard unit of Monte-Carlo time, called the Monte-Carlo step per site MCSS. The time unit MCSS is defined as the time in which an L^2 number of spins (randomly chosen) are updated. The units of magnetic field strength and temperature are respectively J and $\frac{J}{k}$. Each dynamical state, at any temperature T, of Ising ferromagnet under the influence of propagating magnetic field is achieved by slowly cooling the system with small changes in temperature and keeping the system for a sufficiently long time at that particular temperature. The various steady state behaviors are now measured in terms of some dynamical variables and quantities. We may also start from another initial spin configuration where *most* of the spins are either *up* or *down*. This configuration corresponds to the very low temperature ordered state. At very low temperatures thermal fluctuations are very little. As a result the cooperative energy binds the ferromagnetic spins at a particular value; either $+1$ or -1. Then any dynamical state is achieved by heating the system slowly i.e. by rising the temperature in small increments in each step. Results would be the same in both the cases. (We will stick to the first choice henceforth throughout this thesis.)

Results:

Depending upon the amplitude of the magnetic field wave and the temperature two distinct phases: namely *Pinned* phase and *Propagating* phase are observed in steady state. *Figure 2.1* shows the dynamical phases. These are the snapshots of the spin

configuration.

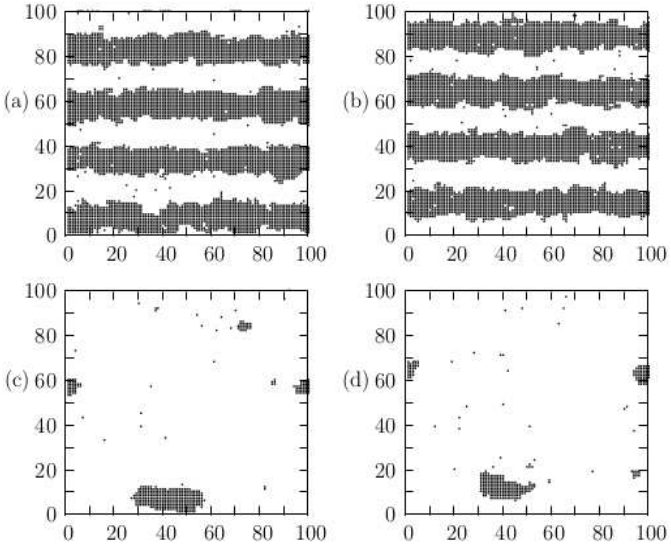

Figure 2.1: The motion of spin-clusters of down spins (shown by *black dots*), swept by propagating magnetic field wave, for different values of (**a**) Time = 100100 MCSS, $T = 1.5$ and $h_0 = 0.6$ (**b**) Time = 100125 MCSS, $T = 1.5$ and $h_0 = 0.6$ (**c**) Time = 100100 MCSS, $T = 1.26$ and $h_0 = 0.6$ (**d**) Time = 100125 MCSS, $T = 1.26$ and $h_0 = 0.6$. This figure is provided by courtesy of M. Acharyya [10].

Here in this study the linear dimension of the lattice is taken to be $L = 100$ and the magnetic field amplitude, frequency and wavelength of the propagating wave are respectively $h_0 = 0.6$, $f = 0.01$ and $\lambda = 25$. It is observed that band like clusters of up and down spins are formed in this phase which move coherently with the propagating magnetic field wave. The propagation of spin strips in the y- direction is clearly shown in the *figures 2.1*(**a**) & *2.1*(**b**), which are the typical spin configurations at times $t =$ 100100 $MCSS$ and $t = 100125$ $MCSS$ respectively. For a given value of h_0, f and λ, the propagating phase is formed above the dynamical transition temperature, whereas the pinned phase is formed below the dynamical transition temperature. Most of the spins are pinned towards a particular direction; either up or down (here it is up; the black dots in the *figures 2.1* represent the down spins) in this phase. The above snapshots of pinned phase are taken at temperature ($T = 1.26$) and that of propagating phase are taken at temperature ($T = 1.5$).

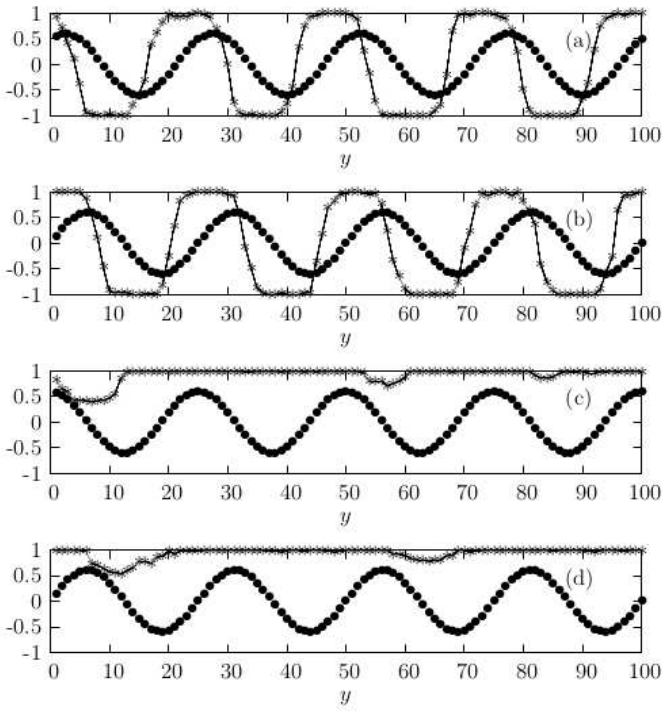

Figure 2.2: The propagation of field (•) and the line magnetization (∗) for various values of (**a**) Time = 100100 MCSS, $T = 1.5$ and $h_0 = 0.6$ (**b**) Time = 100125 MCSS, $T = 1.5$ and $h_0 = 0.6$ (**c**) Time = 100100 MCSS, $T = 1.26$ and $h_0 = 0.6$ (**d**) Time = 100125 MCSS, $T = 1.26$ and $h_0 = 0.6$. This figure is provided by courtesy of M. Acharyya [10].

Because of higher thermal fluctuation at high temperatures, ferromagnetic spins eventually follow the magnetic field oscillations. The line magnetization $m(y,t)$, at any instant, is defined by the *equation 2.4*.

$$m(y,t) = \frac{1}{L}\int s^z(x,y,t)\,dx, \tag{2.4}$$

It has the same periodicity, in time (with period $T = \frac{1}{f}$) as well as in space (with period λ), with that of the propagating magnetic field wave. This may be seen in the *figure 2.2(***a***)* and *figure 2.2(***b***)*. In lower temperature the magnetic field energy is insufficient to break the mutual cooperative strength and the ferromagnetic spins bind each other contributing to nonzero value of line magnetization. As a result the line magnetization lost the spatio-temporal periodicity, which is shown in the *figure 2.2(***c***)* and *figure 2.2(***d***)*. The response of the spins to the magnetic field oscillations may not be immediate, rather

it lags in time due to their cooperative interactions. Also it is seen from these figures that in the high temperature phase, line magnetization oscillates symmetrically about $m(y) = 0$ line; thus it is also called the *symmetric phase*. In contrast to it, we see no oscillation of line magnetization about $m(y) = 0$ line at lower temperatures. This phase is identified as the *symmetry-broken phase*.

The *Order parameter* Q for this dynamical phase transition may be defined as the time averaged magnetization per site over a complete period of magnetic field oscillations which is given as follows:

$$Q = \frac{f}{L} \oint\int m(y,t)\, dy\, dt. \tag{2.5}$$

Because of symmetric oscillation of $m(y,t)$ at higher temperatures the value of Q is zero, while it takes nonzero values at lower temperature where the value of $m(y,t)$ is also nonzero. The variation of order parameter Q and other steady state dynamical quantities are shown in *figure 2.3*. $\frac{dQ}{dT}$, $\langle(\delta Q)^2\rangle$ and C_v represent respectively the temperature derivative of order parameter, the variance of order parameter and dynamic specific heat. The dynamical specific heat C_v is related to the dynamic energy $E(t)$ by the relation $C_v = \frac{dE}{dT}$, where $E(t) = f \oint H(t)\, dt$. These derivatives are calculated numerically by using the 'three points central difference formula' [8]. The steady state values of the above mentioned dynamical quantities are calculated statistically over 1000 different samples. The dynamical transition temperature is determined from the peak (or dip) positions of these dynamical quantities in their respective temperature variations. It is evident from these variations that the dynamic transition temperature (T_d) decreases with the increase in magnetic field amplitude (h_0). For $\lambda = 25$, the transition occurs at $T_d = 1.88$ and $T_d = 1.29$ for $h_0 = 0.3$ and $h_0 = 0.6$ respectively. Collecting more such values of T_d for different values of h_0, the comprehensive phase boundary can be drawn (see *figure 2.3*).

Again, the spatial variation of the magnetic field also has effects on the transition temperature. The dynamical transition also depends on the wavelength of the propagating magnetic field wave. *Figure 2.4* shows the wavelength dependence of the dynamical transition temperature for two different values of wavelength ($\lambda = 25$ and $\lambda = 50$). It is clearly seen from the temperature variations of the steady state dynamical quantities that the transition temperature is low for lower values of wavelength (with fixed value

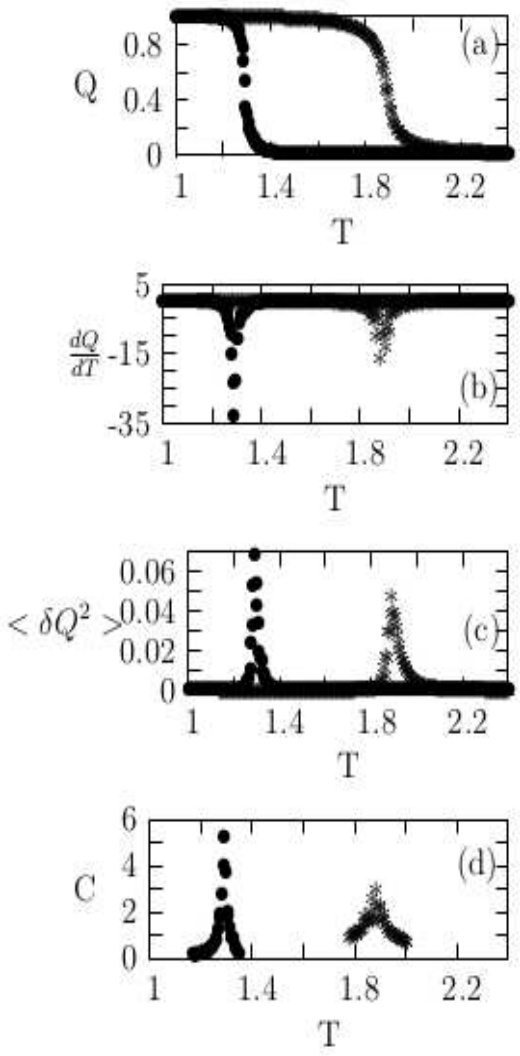

Figure 2.3: The temperature (T) dependence of the (**a**) Q, (**b**) $\frac{dQ}{dT}$, (**c**) $\langle(\delta Q)^2\rangle$ and (**d**) C, for two different values of h_0 for *propagating* magnetic field wave having $f = 0.01$ and $\lambda = 25$. In each figure, $h_0 = 0.3$ ($*$) and $h_0 = 0.6$ ($\bullet$). This figure is provided by courtesy of M. Acharyya [10].

of h_0). To be precise, the transition temperatures are $T_d = 1.88$ and $T_d = 1.94$ for $\lambda = 25$ and $\lambda = 50$ respectively, where $h_0 = 0.3$. Thus, for this reason, the dynamical phase boundary in the $T_d - h_0$ plane shrinks inward (region of lower T_d and h_0) as the wavelength of the propagating magnetic field wave decreases (see *figure 2.5*).

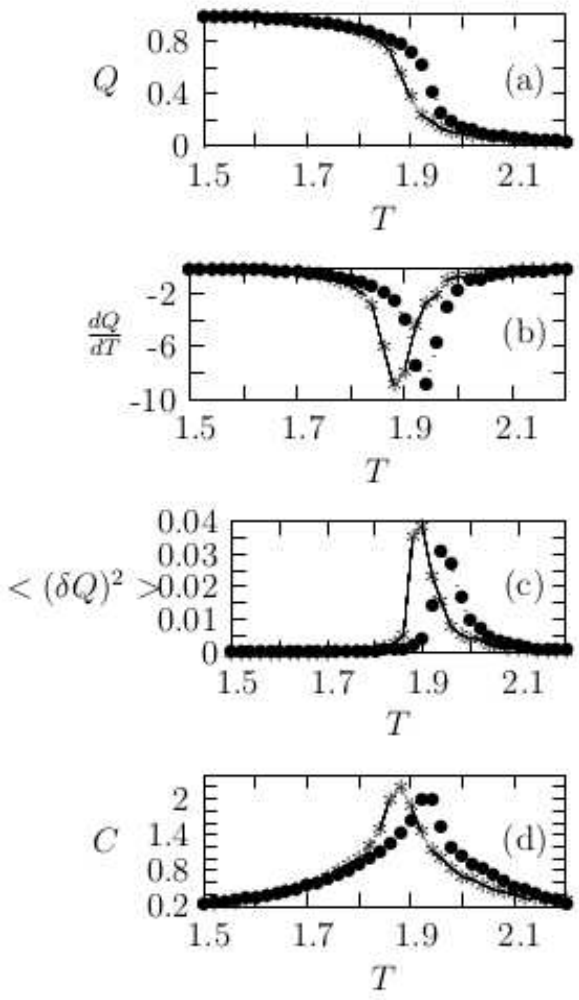

Figure 2.4: The temperature (T) dependence of the (**a**) Q, (**b**) $\frac{dQ}{dT}$, (**c**) $\langle(\delta Q)^2\rangle$ and (**d**) C, for two different values of λ for *propagating* magnetic field wave having $f = 0.01$ and $h_0 = 0.3$. In each figure, $\lambda = 25$ ($*$) and $\lambda = 50$ ($\bullet$). This figure is provided by courtesy of M. Acharyya [10].

In *figure 2.6* it is seen that the peak height of the quantity $L^2\langle(\delta Q^2)\rangle$ near T_d increases as system size L increases. The figure is drawn for two different values of L; viz. $L = 50$ and $L = 100$. This result is quite conclusive, as this shows that there exists a diverging length scale near transition temperature associated with the dynamic phase transition.

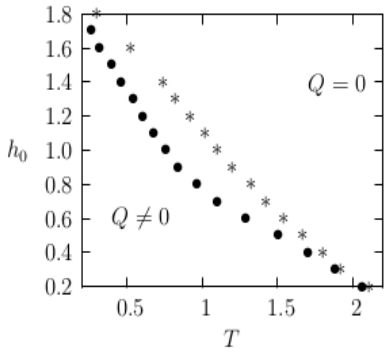

Figure 2.5: The phase diagram for dynamic phase transition by propagating magnetic field wave for two different values of wavelengths, $\lambda = 25$ ($\bullet$) and $\lambda = 50$ ($*$). Here, $f = 0.01$. This figure is provided by courtesy of M. Acharyya [10].

It is noteworthy that this method was employed successfully [9] in the Ising ferromagnet, driven by oscillating (but non propagating) magnetic field, where the existence of diverging length scale associated with the dynamic phase transition was shown.

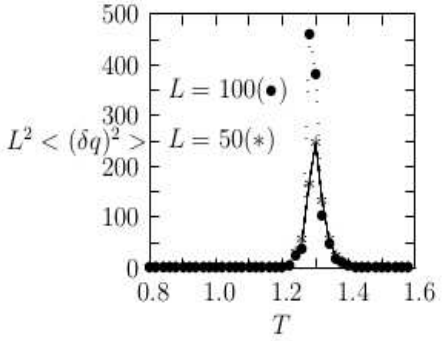

Figure 2.6: The plot of temperature (T) versus $L^2\langle(\delta Q)^2\rangle$ for different system sizes (L). Here, $h_0 = 0.6$, $\lambda = 25$ and $f = 0.01$. This figure is provided by courtesy of M. Acharyya [10].

2.2.2 Response to standing magnetic wave:

Now, let us see the effect of different form of magnetic wave, used as perturbing field, on the nonequilibrium phase transition of an Ising ferromagnet. In this section, I will discuss on the effect of standing magnetic wave in an Ising ferromagnet. We have seen dynamic patterns of spins in such ferromagnet driven by propagating magnetic wave [10] in the earlier *section 2.2.1.* More such dynamic phase transition and pattern formation has been observed in Ising ferromagnet [11, 12] recently. Here, I intended to know how these dynamical patterns as well as steady state behaviors of spins change with such a different form of wave (Standing wave) at finite temperatures. How these changes or differences may be quantified is addressed here in details. In standing magnetic wave, the magnetic field oscillates in loops between two nodes of zero magnetic field. The amplitude has spatial sinusoidal modulation. It seems that a localized modulated time varying magnetic field is driving the ferromagnetic spins which also leads to interesting behavior.

The Hamiltonian for such system may also be written by the *equation 2.1* given by,

$$H(t) = -J\Sigma\Sigma' s^z(x,y,t)s^z(x',y',t) - \Sigma h^z(x,y,t)s^z(x,y,t).$$

The magnetic wave has the general standing wave form given by,

$$h^z(x,y,t) = h_0 sin(2\pi ft)cos(2\pi\frac{x}{\lambda}). \tag{2.6}$$

The specification of all the variables (eg. f, λ, L etc.) are quite similar to that used in the *section 2.2.1.* Here, the standing wave is assumed as linearly polarized parallel to the spins (s^z). Amplitude of the wave is modulated along x-direction only (as given in *equation 2.6.*

Here in the spatial part, $cos(2\pi\frac{x}{\lambda})$ has been considered. The results are same if one uses $sin(2\pi\frac{x}{\lambda})$ instead.

Monte-Carlo Simulation:

The standard *Monte-Carlo* method (with Metropolis rule) is used to simulate the spin dynamics of the Ising ferromagnet. I have taken a lattice of $L \times L$ dimensions over which spins are arranged. Here the boundary condition is set *open.* Unlike in periodic boundaries where translational invariance is preserved, this kind of boundary condition

is used to see the effects of the boundaries [13] beyond which there is no correlation between spins; i.e. the value of spins at any lattice site is not repeated beyond the boundary, which may be the end of the system in reality. The initial configuration of spins corresponds to the very high temperature disordered state where 50 % of total spins are in up ($s^z(x, y, t) = +1$) state and the rest are in down ($s^z(x, y, t) = -1$) state. We may also take another initial configuration where most of the spins are either up or down; the configuration corresponds to the low temperature ordered state. The results would be the same. The system is now cooled in steps of small changes in temperature. The system is kept in a heat bath of constant temperature for a sufficiently long time so as to achieve the nonequilibrium steady state behavior. Once the nonequilibrium steady state is achieved, various dynamical quantities are calculated to detect the dynamical phase transition from the high temperature *Symmetric* phase to the low temperature *Symmetry-broken* phase. Flippings of spins happen at Metropolis rate at a particular temperature. This is given by the *equation 2.3* :

$$W(s^z \to -s^z) = Min[exp(-\Delta E/kT), 1].$$

Results:

In any dynamical steady state at a temperature (T) the distribution of up-spins and down-spins in the lattice depends upon the temperature and the strength of magnetic field. At low temperatures thermal fluctuations decrease and the spin-spin interaction leads most of the spins to orient parallel to each other giving rise to a net effect of magnetization. Two distinct phases (see *figure 2.7*) namely, *Pinned* and *Oscillating spin clusters* are identified in the steady state. While the pinned phase is formed below certain transition temperature called the *dynamic transition temperature* (T_d), the oscillating spin clusters phase is formed above this temperature.

In the pinned phase, most of the spins orient in some preferred direction, i.e. either upward or downward. Here, the value of the temperature and amplitude of field are such that the local oscillations of field are incapable of flipping the spins within the time scale of its time period. Whereas in the oscillating spin clusters phase, alternate bands of up and down spins of bandwidth $\frac{\lambda}{2}$ are formed parallel to the y direction. Here, the field amplitude is strong enough to flip the spins within the time scale of time period

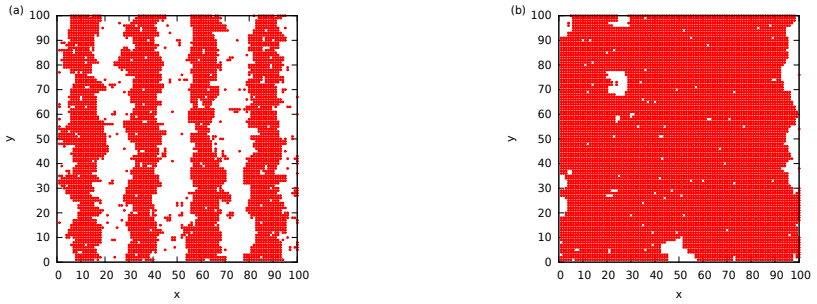

Figure 2.7: (Color online) Dynamical lattice morphology for frequency $f = 0.01$ and field amplitude $h_0 = 0.6$. (**a**) Oscillating spin clusters phase (temp. $T = 2.0$), (**b**) Pinned phase (temp. $T = 1.5$). In these figures red dots denote up spin states.

of standing wave. This is the dynamically disordered phase with nearly 50% of spins in the up state. The alternate bands of spins oscillate, i.e. reverse in direction in every half time period of oscillation, with the same period as that of the magnetic field wave. Thus, oscillation of spin bands form standing wave instead of showing of propagation as we observed in the previous studies done with propagating magnetic wave (*section 2.2.1*). At low temperatures and for small values of the amplitude of the magnetic field wave, the probability of spin flip becomes very small, leading to the dynamical pinned phase. But for sufficiently high values of temperature and the field amplitude the probability of spin flip increases and the ferromagnetic spins effectively follow the spatio-temporal variation of the standing magnetic field wave and this eventually leads to an oscillating spin bands phase. *Figure 2.7* shows typical snapshots of two different phases. We see in these figures the definite patterns of spins in pinned as well as in oscillating spin bands phases. Here lattice dimension is $L = 100$. In this study, the frequency of the magnetic wave is kept fixed at 0.01 $(MCSS)^{-1}$ and the value of wavelength is $\lambda = 25$ lattice units (lu). The *dynamic Order parameter* (Q) for this dynamic phase transition is defined as the *time averaged magnetization per lattice site over a full cycle of the magnetic field oscillations of standing magnetic wave*, i.e.

$$Q = \frac{f}{L} \oint \int m(x,t)\, dx\, dt. \tag{2.7}$$

Here $m(x,t)$ is the instantaneous value of *line magnetization* (*Eqn.2.8*) at site x. It is defined as the average value of spin variable (s^z) over all sites along y direction, at any instant at a lattice site x (direction is a choice depending upon the choice of the modulation of the standing wave (*Eqn.2.6*), which is along x- direction here). It is given

as follows:

$$m(x,t) = \frac{1}{L}\int s^z(x,y,t)\,dy. \tag{2.8}$$

The value of order parameter in low temperature pinned phase is large because of the parallel orientation of most of the spins in the ferromagnet. In the oscillating spin clusters phase, the order parameter is nearly zero for a pair of alternate spin clusters contribute a complementary sum (nearly equal in magnitude and opposite in sign) to the value of order parameter. The variation of the dynamic order parameter with temperature is shown in *figures 2.8(***a***)* and *2.9(***a***)*. As the ferromagnet is cooled below a certain temperature,

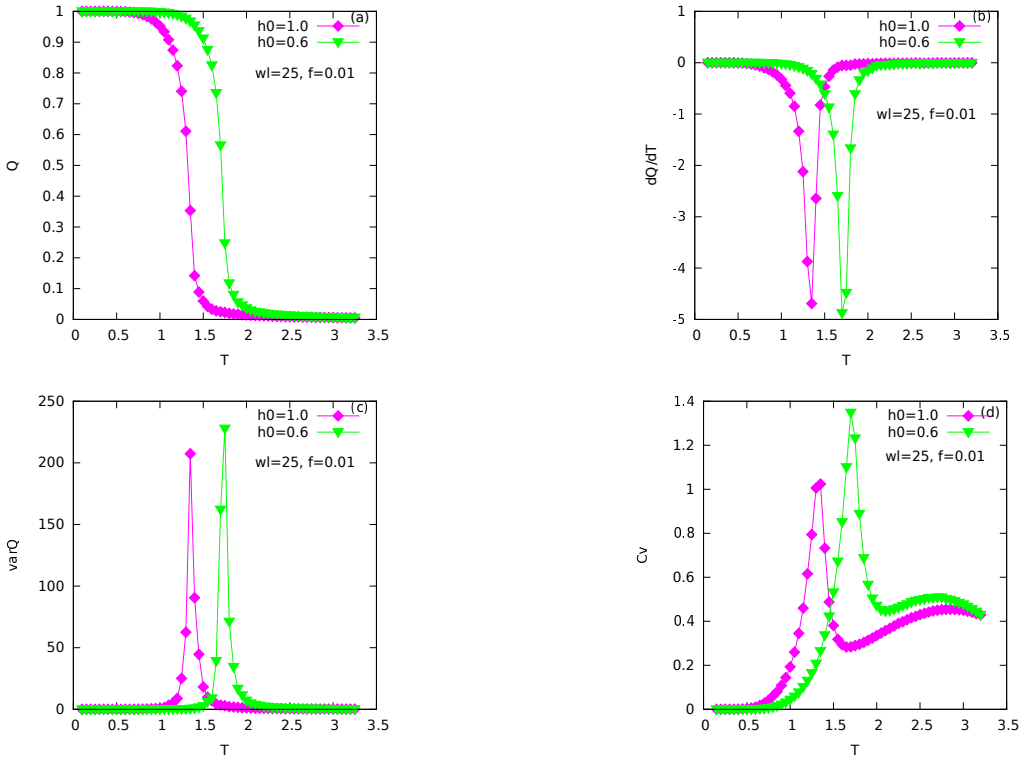

Figure 2.8: (Color online)Temperature (T) variations of **(a)** Q, **(b)** $\frac{dQ}{dT}$, **(c)** $L^2\langle(\delta Q)^2\rangle$ and **(d)** C_v for two different values of standing magnetic field amplitude h_0. Here Q is the order parameter, L is the lattice size and C_v is the specific heat. Symbols ($\triangledown$) & ($\diamond$) represent $h_0 = 0.6$ & $h_0 = 1.0$ respectively. The frequency and the wavelength of the standing wave are respectively 0.01 $MCSS^{-1}$ and 25 lattice units. The size of the lattice is 100×100.

the dynamic transition temperature, the value of order parameter increases from nearly zero to a large value in the pinned phase generating the dynamic phase transition. The nonequilibrium dynamic transition is detected from the sharp *dip or peaks* in the thermal variation of the dynamical variables $\frac{dQ}{dT}$, ($varQ = L^2\langle(\delta Q)^2\rangle$) and $C_v = \frac{dE}{dT}$ respectively near the transition temperature. $E = f\oint\{-J\Sigma\Sigma' s^z(x,y,t)s^z(x',y',t)\}\,dt$ is the average

dynamic cooperative energy per spin state of the system (i.e. the system energy without considering the field energy). These are the same quantities as mentioned in the earlier *section 2.2.1.* The variations of these above mentioned dynamical variables with temperature are shown in two sets of *figures (2.8 & 2.9)* for two different values of magnetic field amplitude ($h_0 = 0.6$ & 1.0) corresponding to the two different values of wavelength ($\lambda = 25$ & 50).

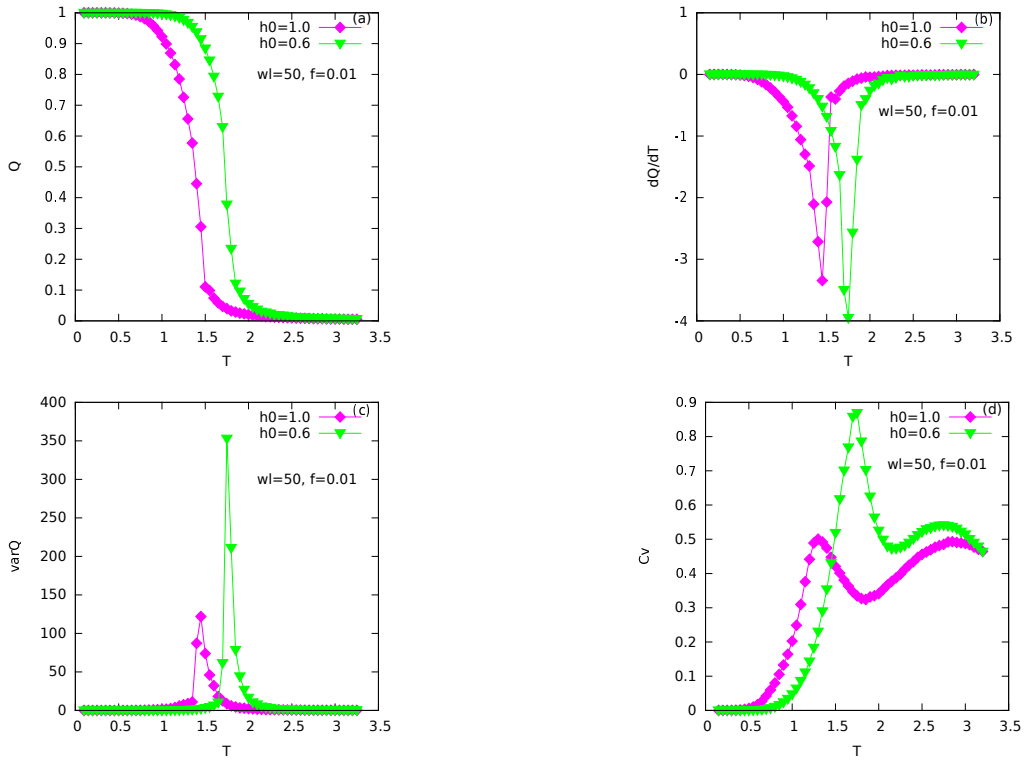

Figure 2.9: (Color online)Temperature (T) variations of **(a)** Q, **(b)** $\frac{dQ}{dT}$, **(c)** $L^2\langle(\delta Q)^2\rangle$ and **(d)** C_v for two different values of standing magnetic field amplitude h_0. Here Q is the order parameter, L is the lattice size and C_v is the specific heat. Symbols ($\triangledown$) & ($\diamond$) represent $h_0 = 0.6$ & $h_0 = 1.0$ respectively. The frequency and the wavelength of the standing wave are respectively 0.01 $MCSS^{-1}$ and 50 lattice units. The size of the lattice is 100×100.

It is worthy to mention here that the *total length* of simulation, in this particular study, continued for 2×10^5 $MCSS$ for each temperature value. Initial (0.5×10^5 $MCSS$) transient data are discarded to achieve steady state. Thus the ferromagnet is kept in constant temperature bath through 1.5×10^5 $MCSS$ to measure the steady state dynamical quantities at any temperature T. Actually all dynamical quantities are calculated by averaging over 1.5×10^3 no. of cycles of magnetic oscillation during such time. Here a full cycle requires 100 $MCSS$ for $f = 0.01$ $MCSS^{-1}$. Temperature is cooled in small steps

of $\Delta T = 0.05\ J/k_B$. This particular choice is a compromise between the computational time and the precision in measuring the transition temperature.

It is evident from the above figures that dynamic phase transition occurs at lower temperatures for higher values of field amplitude. As the field amplitude increases, probability of spin flip towards the field direction also increases. So, when the oscillating magnetic field reverses its direction at every interval of half time period, ferromagnetic spins try to follow the field and the mutual cooperative energy becomes insufficient to keep the spins locked at a particular value ($+1\ or\ -1$), leading to lowering the transition temperature. Also, transition occurs at lower temperatures for smaller wavelengths of magnetic field wave (having fixed values of magnetic field amplitude and frequency). This is reflected in the phase boundary drawn in the ($h_0 - T_d$) plane for two wavelengths ($\lambda = 25\ and\ 50$ lu); see *figure 2.10*. The phase boundary shrinks inward (towards

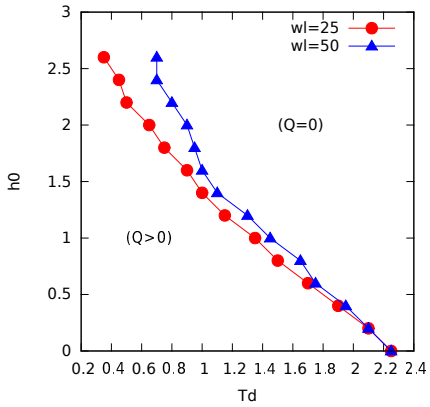

Figure 2.10: (Color online)Phase diagram (dynamic transition temperature T_d vs. field amplitude h_0) for two different wavelength ($\lambda = 25$ (•) & 50 (△)) of the standing magnetic field wave. The frequency of the standing wave is $f = 0.01\ MCSS^{-1}$.

lower values of temperature and magnetic field) for smaller wavelength. For shorter wavelengths of magnetic wave, the variation of magnetic field in space within the lattice is faster relative to the magnetic wave having longer wavelengths. There are more nodes of magnetization (zero values of magnetization) in a lattice for smaller wavelength standing magnetic wave. At the nodes, the strength of magnetic field is minimum. Hence, the probability of spin flip is higher at these nodes due to thermal fluctuations. With the increase in the number of nodes (due to shorter wavelength) flipping of spins in the whole lattice is rather higher. As a result the absolute value of magnetization also becomes

smaller. These leads to a lower value for dynamic transition temperature. The result is consistent with the results obtained previously with propagating and standing magnetic wave using periodic boundary conditions.

The nature of transition looks similar to that observed in the case of propagating magnetic field wave; *section: 2.2.1.* However, the phases formed in the case of standing wave are different from each other. In the *figures 2.11* the spatial (x) variation of line magnetization is shown at four instants at equal intervals within a period. These, collectively, describe the periodic variation of the dynamical quantity. It is clear from

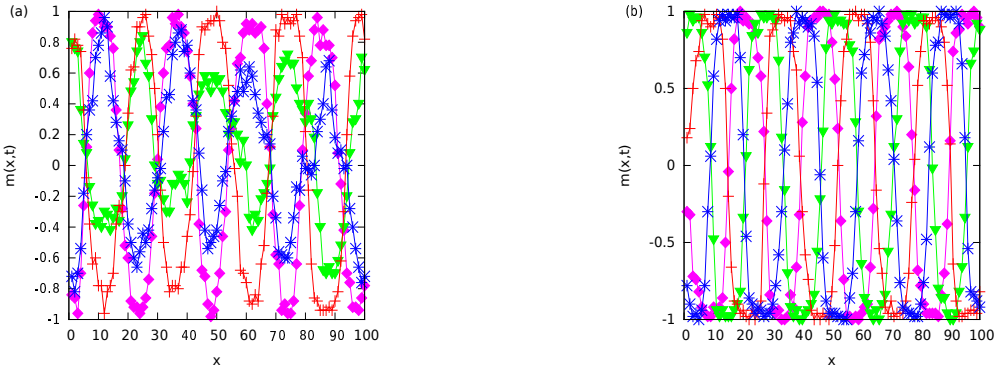

Figure 2.11: (Color online) Periodic variation of line magnetization $m(x,t)$ at different lattice sites (x); for (a) *standing wave*, (b) *propagating wave* in disordered phase, temperature $T = 2.00\ J/K$. Different symbols represent different times ($\diamond$) at 199900 $MCSS$, ($\triangledown$) at 100925 $MCSS$, ($+$) at 199950 $MCSS$ and ($*$) at 199975 $MCSS$, where time period is 100 $MCSS$. Here $h_0 = 0.6\ J$, $f = 0.01\ MCSS^{-1}$ and $\lambda = 25\ lu$.

these *figures 2.11* that line magnetizations (*equation 2.8*), at various lattice sites (x), lying between any two consecutive nodes of standing wave, oscillate coherently with different amplitudes and form loops. Whereas it would propagate if the ferromagnet was driven by propagating wave. At the nodes of standing magnetic wave, line magnetization oscillates with minimum (or zero) amplitudes but at the anti-nodes the corresponding amplitude is maximum. In such a case of standing magnetic wave, spins inside a loop oscillate coherently with the oscillation of the local magnetic field, where spins inside two nearest loops oscillate in opposite phase. Actually at nodes i.e. at loop boundaries spins feel the minimum effect of the magnetic field and thus their dynamics are governed by thermal fluctuation. On the other hand, the dynamics of the spins at the anti-nodes are governed mostly by the field. This is shown in *figure.2.12.* The flipping probability of a spin, at any lattice site (x) depends upon the temperature and the local magnetic field

strength. Because of low intensity of the magnetic field at nodes, the probability of spin flip is high there. The peaks at nodes of standing magnetic wave (*figure 2.12*) describes

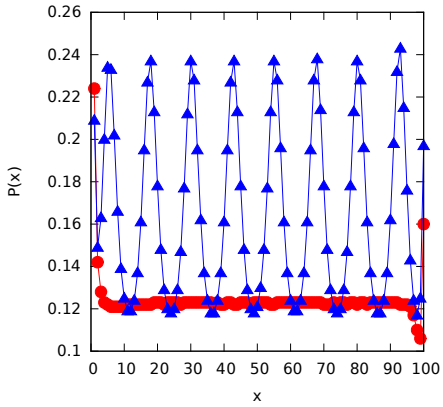

Figure 2.12: (Color online) Probability $P_s(x)$ of spin flips at different lattice sites along x-axis for standing magnetic wave (●) and for propagating magnetic wave (△) respectively in disordered phase, temperature $T = 2.00\ J/k$. Here $h_0 = 0.6\ J$, $f = 0.01\ MCSS^{-1}$ and $\lambda = 25\ lu$.

that the probability of spin flip, over a full period of magnetic oscillation, is quite large at these sites as compared to other lattice sites. Again when the Ising ferromagnet is driven by propagating magnetic field wave the probability of spin flip is quite low at all lattice sites since all spins feel the same magnetic field strength over a full period. This distinguishing characteristic manifests the difference between the dynamical phases in Ising ferromagnet driven by standing magnetic wave and propagating magnetic wave.

Bibliography:

1. B. K. Chakrabarti and M. Acharyya, *Rev. Mod. Phys.* **71** (1999) 847; see also M. Acharyya, *Int. J. Mod. Phys. C* **16** (2005) 1631.
2. M. Acharyya, *Phys. Rev. E* **58** (1998) 179.
3. M. Acharyya, *Phys. Rev. E* **59** (1999) 218.
4. M. Acharyya, *Phys. Scr.* **84** (2011) 035009.
5. M. Acharyya, *J. Magn. Magn. Mater.* **334** (2013) 11.
6. K. Huang, *Statistical Mechanics*, Second Edition, John Wiley & sons Inc, Wiley India edition 2010.
7. K. Binder and D. W. Heermann, *Monte-Carlo Simulation in Statistical Physics*, Springer Series in Solid State Sciences, Springer, New York, 1997.
8. C. F. Gerald, P. O. Weatley, *Applied Numerical Analysis*, Reading, MA: Addison-Wesley, 2006; J. B. Scarborough, *Numerical Mathematical Analysis*, Oxford: IBH, 1930.
9. S. W. Sides, P. A. Rikvold, M. A. Novotny, *Phys. Rev. Lett.* **81** (1998) 834.
10. M. Acharyya, *Acta Physica Polonica B* **45** (2014) 1027.
11. M. Acharyya, *J. Magn. Magn. Mater.* **354** (2014) 349.
12. M. Acharyya, *J. Magn. Magn. Mater.* **394** (2015) 410.
13. H. Park and M. Pleimling, *Phys. Rev. Lett.* **109** (2012) 175703.